ELSEVIER

PII: S0032-3861(97)10156-2

Polymer Vol. 39 No. 19 pp. 4489–4495, 1998

0032-3861/98/$19.00+0.00

Cylindrulitic morphologies in dispersions of polymers and liquid crystals

Andrew J. Lovinger*, Karl R. Amundson and Don D. Davis
Bell Laboratories, Lucent Technologies, Murray Hill, NJ 07974, USA
(Received 17 July 1997; accepted 22 August 1997)

Thin-film mixtures of nematic liquid crystals in a photopolymerizable prepolymer can yield not only the well-known 'polymer-dispersed liquid crystal' droplet morphology but, in different ranges of composition and polymerization temperature, a spherulitic-like morphology (which is more properly described as 'cylindrulitic' because these structures grow as disks about a central defect axis anchored at the film surfaces). These cylindrulites exhibit a variety of important characteristics including our previously described radial inversion wall defects. Growth rates are linear and extremely slow (≤ 1.7 μm/h). Isotropization manifests itself in two stages, first through a non-birefringent band at the cylindrulitic perimeter which tends to spread along the inter-cylindrulitic boundaries. Isotropization in the interior then follows *ca*. 0.1°C higher in temperature and occurs by nucleation and growth of cylindrical non-birefringent domains. There are also indications that encirclement of clusters of cylindrulites by isotropized bands at their perimeter may promote earlier nucleation of isotropic domains in their interiors, as well. The radial inversion wall defects within the cylindrulites generally survive heating and cooling through the isotropization temperature and are impacted in a variety of ways in the vicinity of nucleated isotropic regions: the inversion walls can be redirected to either side of an isotropic domain with or without termination, they can be annihilated at that particular region, or they can remain unaffected.

(Keywords: spherulites; morphology; thin films)

INTRODUCTION

Polymer-dispersed liquid crystals (PDLCs) consist of μm-sized dispersions of nematic liquid-crystal droplets in an amorphous polymer matrix[1–5]. In perhaps the most common manifestation, the liquid crystal has a positive dielectric anisotropy so that it can be aligned by an external electric field. If the ordinary refractive index matches the refractive index of the polymer matrix, the composite film becomes transparent when the droplet director is aligned normal to the film, i.e. when the external field is on. With the field off the droplets are directed according to local forces, yielding a white, scattering appearance. Such PDLC films are therefore under intense interest as potential flat-panel display materials[1–5] and in switchable architectural windows. In this regard they offer advantages over the common liquid-crystal displays because they require no polarizers (which absorb more than half of the transmitted light) or alignment layers. Recently, these PDLCs have also been successfully patterned in the form of gratings[6] for electrically switchable holographic applications[7,8].

One common scheme for preparing PDLC films is by dissolving a mixture of liquid crystals having the appropriate dielectric and thermal characteristics into a compatible photocurable prepolymer[9]. Upon UV curing, phase separation of the liquid-crystal component occurs as a result of polymerization[10–15]. Depending upon the degree of cross-linking of the matrix and the rate of change of its viscosity, the liquid-crystal (LC) component may be rejected in the form of larger or smaller droplets having spherical or non-spherical shapes[13–15]. It is even possible to incorporate over 80% LC in some acrylate matrices, leading eventually to polygonal droplets separated by thin walls of cross-linked polymer[16–18].

In previous work[19,20] we studied the morphology of such PDLCs as a function of radiation dose, composition, and irradiation temperature. We discovered that, over a wide range of compositions and temperatures, the resulting thin films do not consist of phase-separated droplets but of an unexpected spherulitic-like morphology. These two-dimensional 'spherulites' can be area-filling over the full extent of the sample and are usually replete with radially directed defects which we identified as *inversion walls*. These 'spherulites' are specific to samples confined between rigid or flexible surfaces (e.g. glass or plastic) as for typical flat-panel display applications—although no alignment layers or any special treatment are required. They are initiated at $s = +1$ disclination lines whose ends are anchored at the two internal surfaces (or through escaped $s = +1$ disclinations)[19,20]. They result from aligned 'nucleation' and 'growth' of a nematic LC phase within the viscoelastic, partly cross-linked polymer in a manner very similar to spherulitic crystallization of semi-crystalline polymers[21,22]. However, they are not true spherulites, since they do not grow as spheres but rather as disks or cylinders about a central axial defect line anchored at the film surfaces. They are thus more properly described as 'cylindrulites' and will be referred to as such in this paper, in which we examine their morphologies further by concentrating on their growth and thermal behaviour and uncovering new phenomena associated with their nematic–isotropic transition.

* To whom correspondence should be addressed

EXPERIMENTAL

The materials were the same as used previously[19,20]. The matrix is a commercial photopolymerizable mixture (NOA65) obtained from Norland Products, Inc. (New Brunswick, NJ, USA), and contained primarily trimethylolpropane diallyl ether, trimethylolpropane tristhiol and a diisocyanate ester[10]. The liquid-crystal component is a eutectic mixture of cyanobiphenyls and -triphenyls (Merck Industrial Chemicals E7) having a nematic–isotropic transition temperature in the region of 61–62°C. To avoid premature polymerization, the prepolymer mixture was kept in the dark and handled under diminished illumination during processing. The materials were blended just prior to polymerization, sandwiched between thin cover slips to yield 12–18 μm thick films, and irradiated with a 100-W Hg lamp at room temperature to doses of 5–6 J/cm^2. Morphological investigations were conducted with a polarizing microscope. A Mettler FP 5/52 microscope heating stage was used to control the temperature during the thermal studies.

RESULTS AND DISCUSSION

The two basic types of morphology encountered in these PDLCs are shown in *Figure 1*. Samples containing 65 wt.% LC yield the well-known dispersion of liquid-crystal droplets in the cross-linked matrix (*Figure 1a*), while those containing 35% LC exhibit typically the cylindrulitic morphology (*Figure 1b*) that is the subject of this investigation. The cylindrulite of *Figure 1b* shows especially clearly the radial striations characterizing this morphology. We have shown[19,20] that these striations represent 'inversion wall defects' through which the nematic director is rotated in the plane by 180°. We also found that these are always initiated at $s = +1/2$ disclinations (never at $s = -1/2$); they can be terminated at $s = -1/2$ counterparts (in which case a non-birefringent closed loop is seen between crossed polars) or extend all the way to the cylindrulitic perimeter.

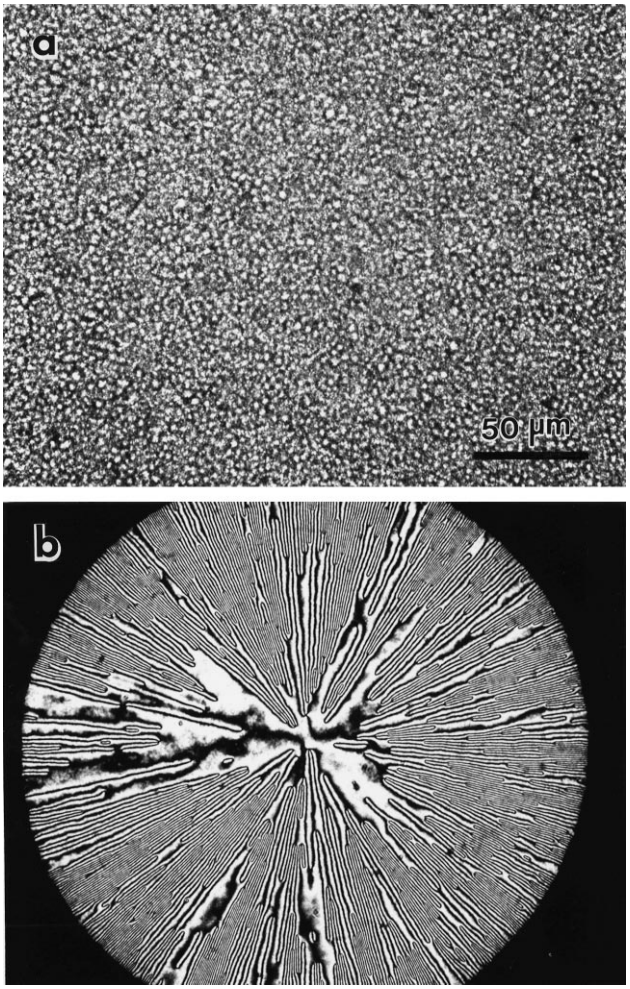

Figure 1 Typical morphologies of PDLC samples containing (a) 65 and (b) 35% liquid-crystal component by weight following photopolymerization at room temperature. Both polarizing micrographs are recorded at the same magnification

Growth of these cylindrulites is monitored in *Figure 2* at successive stages following their initiation, which occurs after photopolymerization. *Figure 2a*, obtained at 22 h after photopolymerization shows well-developed negatively birefringent structures exhibiting full cylindrical symmetry. The larger ones in this field (e.g. number 1) appeared almost immediately after UV irradiation. Inversion walls are visible in all cylindrulites. In many cases these are seen to be initiated at the 'nucleus', implying that the entire cylindrulite was nucleated at an $s = N + 1/2$, rather than at an $s = +1$. disclination line (where N is the number of inversion lines). At much longer times (e.g. 54 h as in *Figure 2b*) the field is almost completely filled with these cylindrulites in a manner entire analogous to the case of spherulitic growth of semicrystalline polymers. *Figure 2c* (recorded at 78 h) was selected to monitor the case of cylindrulites that were initiated long after the photopolymerization and that are also growing in a region of 'confined nutrient'. One such cylindrulite is numbered '3' and is seen in *Figure 2d* to be growing within a very small region commensurate to the average size of preexisting cylindrulites. Such confined regions are known[21,22] in the semicrystalline-polymer case to be rich in non-crystallizable (or poorly crystallizable) 'impurities' that are being rejected by the growing spherulites and have thus been trapped in these confined spaces; as a result, spherulitic growth in these regions is substantially retarded.

The actual growth rates of these three numbered cylindrulites (representing the cases of initiation immediately after UV irradiation and at early and late stages, respectively) are shown in *Figure 3*. In general, the cylindrulites grow linearly, but exceedingly slowly: those initiated in the initial and early stages grow at 1.73 and 1.68 μm/h, respectively, while the one that grew in the late stage did so at a significantly reduced rate (1.32 μm/h). Therefore, even though this is not a case of crystal growth (as in polymers), the analogy in the effects of confined environments is seen to hold. The 'rejected' species that seem to accumulate in the confined region and retard accretion of the liquid-crystal molecules must be short chains of the polymer (i.e. those that are not attached to the polymer network). It is interesting to note that morphological effects of this enrichment in rejected polymer are not apparent in *Figure 2* (as will be discussed later also in terms of isotropization behaviour). However, as growth continues, coarsening of growth fronts and distortion of inversion walls is commonly seen (as illustrated in Fig. 15(d) of Ref. [19]); again, such effects are reminiscent of spherulitic crystallization in polymers even though the underlying phenomena are quite different.

The isotropization behaviour of these LC cylindrulites is examined with the aid of *Figure 4*, where successive stages in the nematic-to-isotropic transition (*Figure 4a–c*) and in the subsequent isotropic-to-nematic transition (*Figure 4d*)

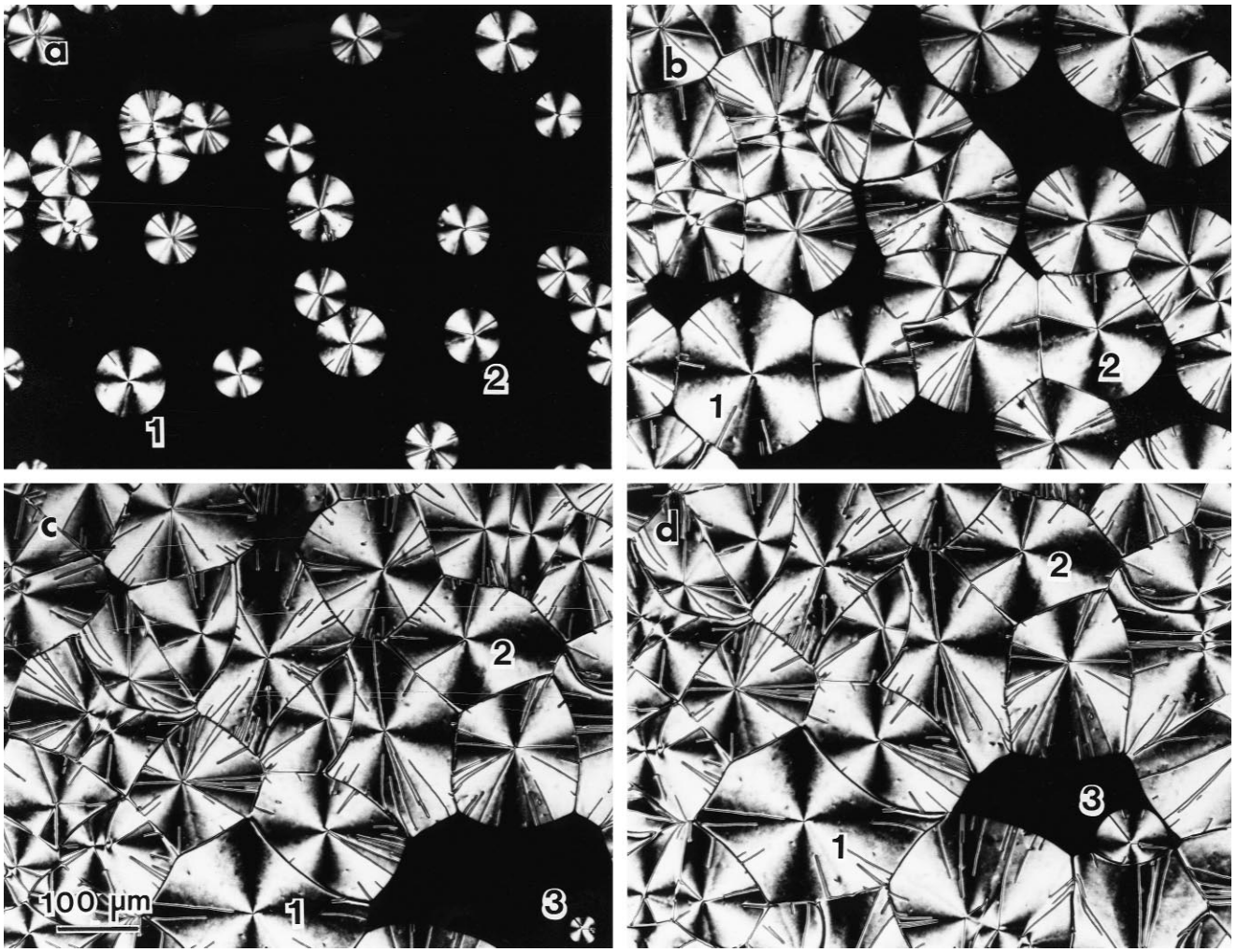

Figure 2 Polarizing micrographs of a PDLC sample containing 25% liquid- crystal component by weight recorded at different times during growth following photopolymerization at room temperature using a dose of 5.6 J/cm^2

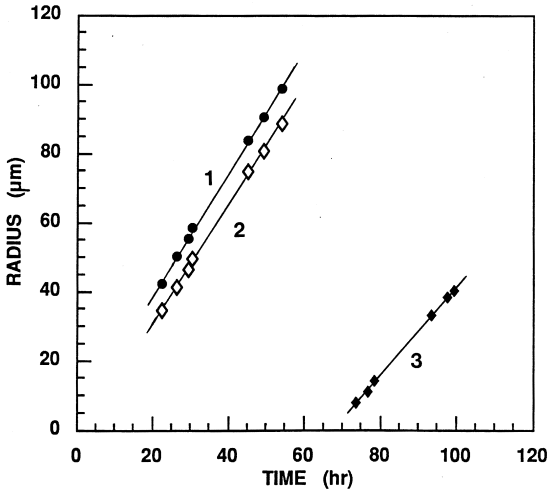

Figure 3 Growth rate of cylindrulites in *Figure 2* that had been initiated immediately after UV photopolymerization (1), at an early stage thereafter (2), and at a late stage in a confined region for growth (3)

are recorded for the sample of *Figure 2*. Here we see for the first time a major difference between these LC cylindrulites and the widely studied polymer spherulites: the former do not undergo isotropization uniformly as the latter usually do (other than, of course, in cases of coexistence of different crystallographic polymorphs or heating-induced phase transitions). In fact, the LC cylindrulites are seen to disorder by nucleation and growth of isotropic regions that appear to be randomly distributed within them. It should be noted that even cylindrulite 3, which had been initiated long after all the others in that field and which had grown in a confined region, does not differ in its isotropization behaviour. This implies that the effects of the amorphous polymer in slowing down growth do not extend to lowering the nematic-to-isotropic transition. This is a major difference from polymers, but one that can be understood by the fact that here there is no crystallographic lattice enriched in, say, lower-molecular-weight or branched polymer chains that is undergoing melting, but rather a chemically distinct and already partly disordered phase that is undergoing further disordering. This uniformity in isotropization behaviour is somewhat deceiving because most of the cylindrulites are of similar (and not very large) size—average of 100–150 μm. For much larger cylindrulites, e.g. > 400 μm, for which accumulation of amorphous polymer chains has increased substantially during extensive radial growth, nucleation of isotropic 'patches' during heating begins near the cylindrulitic periphery (a striking case was seen in Fig. 16(c) of Ref. [19]); even here, the non-birefringent patches near the periphery of the larger cylindrulites are slightly larger than those near their centres.

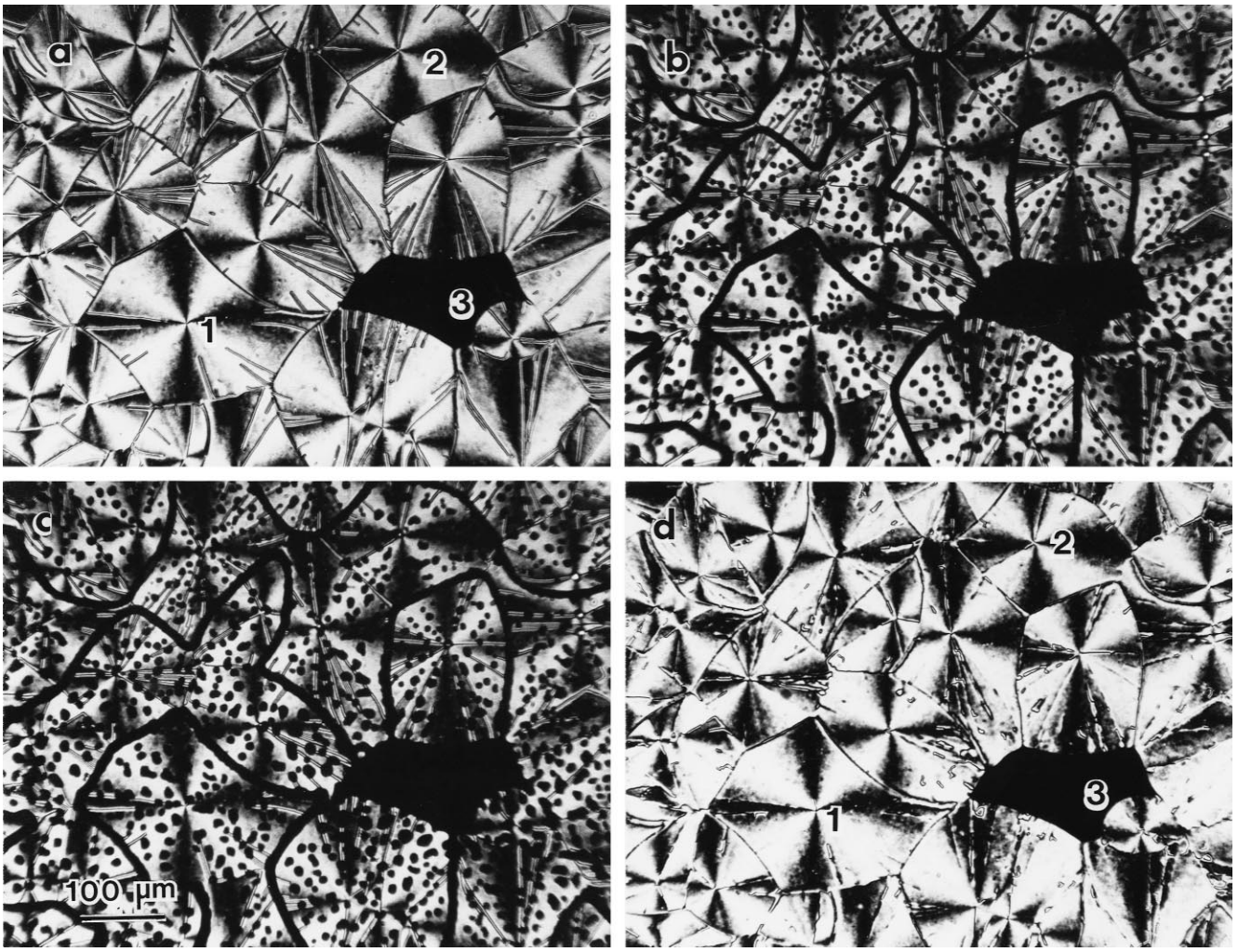

Figure 4 Isotropization of cylindrulites of *Figure 2* during heating, and subsequent transition to the nematic phase upon subsequent cooling. (a) Sample heated from room temperature to (a) 61 and (b) 62°C; (c) sample kept at 62°C for 5 min; (d) sample cooled to room temperature after 15 min at 70°C

Moreover, isotropization is also seen here to be initiated at the inter-cylindrulitic boundaries; this appears at first to occur randomly—some boundaries disorder while others do not. This irregular manifestation might conceivably have been a result of slight differences in the growth history of one of the constituent cylindrulites intersecting at a common boundary. However, this is not the case because then all the edges of that particular cylindrulite should have disordered—and this is seen only very rarely, e.g. for a single cylindrulite in *Figure 4b* (located near the top right). What appears, instead, to be occurring is that once isotropization has been initiated at any particular point in an inter-cylindrulitic boundary it travels along that boundary and then beyond along other contiguous boundaries, taking random paths at branch points where three cylindrulites meet. This is clearly observed in *Figure 4b*; we have very rarely seen a case where this process has stopped after only a single inter-cylindrulitic segment. It is also noteworthy that the initiation of this process takes place preferentially where isotropic material is already present, e.g. at regions that had not yet grown into the cylindrulitic nematic phase. This is evident in the same figures, where almost all of the boundaries ending in the 'confined' region adjacent to cylindrulite 3 have disordered. It is, of course, not surprising that isotropic pools serve as nuclei to initiate transformation to that phase along the 'weakest' path, namely at the intersections between the nematic cylindrulites where surface stresses and defects would lower the barrier for such a transformation.

We can determine whether the two isotropization loci (inter- or intra-cylindrulitic) are initiated simultaneously or not by very slow heating and isothermal studies at temperatures near the transition region. *Figure 5a* shows a sample held at 61.8°C in which disordering has just started at some cylindrulitic perimeters (this actually begins as soon as that temperature is reached). While remaining at 61.8°C for very long periods of time (*Figure 5b* and *Figure 5c*), the width of the isotropized perimeter is seen to increase only slightly (also the point made above about the meandering continuity of these inter-cylindrulitic isotropic regions through many successive branch points is clearly confirmed). However, no disordering has occurred within the interior of the cylindrulites even after more than an hour at this temperature. Yet, a rise by only 0.1°C (*Figure 5d*) causes nucleation of this process in the interior of all cylindrulites. We therefore conclude that the inter-cylindrulitic phase transformation occurs first, probably because the large nemato-elastic strain at the boundaries serves to raise the energy of the nematic phase or because of a relatively high polymer concentration at the boundaries.

A very unusual aspect of these cylindrulites is that they are complicated by slight variations in phase behaviour that

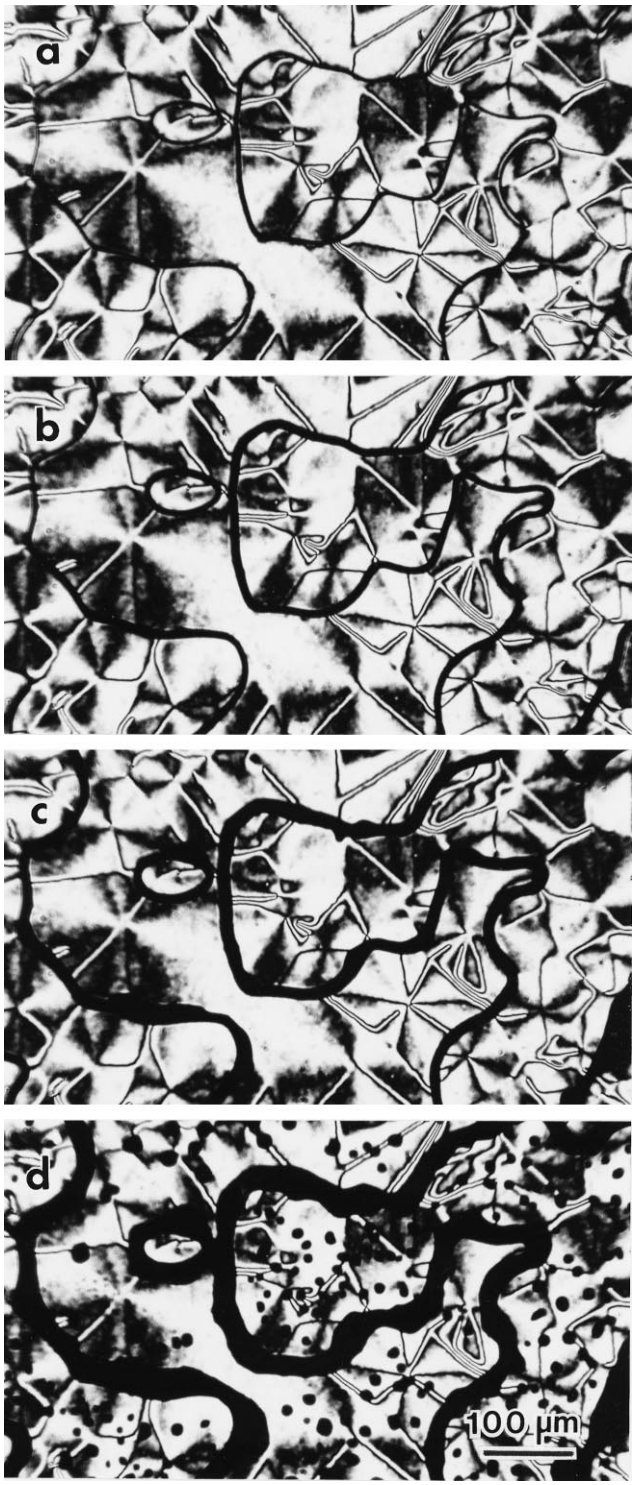

Figure 5 Effects of isothermal treatment at the nematic-to-isotropic transition region. Sample of 25% LC at 61.8°C for (a) 23, (b) 40, and (c) 72 min; (d) sample at 61.9°C for 1 min

are not a priori predictable. One example of this is shown in *Figure 6a–c*, where a field of cylindrulites is heated to the isotropization temperature as in *Figure 4*. Here, however, it is clear that individual cylindrulites (or clusters of these) disorder at slightly different temperatures. The cluster at the top of *Figure 6c* is seen to be close to full isotropization, followed by the one at the left edge; the central spherulite is next, followed by a number of adjacent ones—but the cluster at the lower right has apparently not even begun this process! Even though the differences in isotropization temperature are small (< 0.2°C), they are very puzzling and we have no definitive explanation for them. Possible causes that are ruled out include thermal or compositional gradients across the field of view or surface effects from the glass surfaces (because individual cylindrulites in contact can melt separately). Also, the birefringence of all cylindrulites is the same, so there are no differences in their thickness nor are they separately confined to only one of the inner glass surfaces. Whatever the cause for the different disordering temperatures, it reflects influences that propagate uniformly throughout each individual cylindrulite—from nucleus to the periphery or vice versa.

We have already shown[19,20] that cylindrulites (including their inversion walls) survive isotropization and reappear upon cooling to room temperature. This phenomenon is in fact a version of 'pseudomorphosis', described in detail for block copolymers by Wittmann et al. [23]. This phenomenon is evident in *Figure 6d*. However, inversion walls can be affected in a number of ways by adjacent regions of isotropic material, as we can see with the aid of *Figure 7*. There are cases such as numbers 1, 2, and 3 in *Figure 7b* where the inversion wall defect is actually drawn in towards the isotropic region, without any further effect (i.e. no discontinuation or other disruption). Depending upon their relative locations, the inversion wall may be shifted either to the near side or to the far side of the isotropic region (e.g. numbers 3 *versus* 1, respectively). A second case of such interactions involves redirection of the inversion wall *with* termination (numbers 4, 5). A third type of effect occurs when the isotropic region is centred directly on the inversion wall (e.g. numbers 6 and 7); in this case, the inversion wall defect is seen to be annihilated at that particular spot. Finally, there are cases such as 8, 9, and 10, where there is no apparent effect, i.e. where the inversion wall defect reappears undistorted after cooling. Which of these might occur in any particular case will depend on proximity, extent of disordering and additional factors that are not clearly predictable; for example, of the three isotropic regions numbered 6, 8, and 9 that traverse the same inversion wall region, two have no effect while the third causes localized annihilation.

CONCLUSIONS

The cylindrulitic morphology obtainable in PDLCs exhibits a variety of important characteristics. Growth rates are linear and extremely slow (*ca*. 1.7 μm/h); in confined regions growth is further retarded. Isotropization generally takes place in two stages. First there is localized disordering at the cylindrulitic perimeter, especially where it might be in contact with pre-existing isotropic regions. This disordered band tends to spread along the inter-cylindrulitic boundaries, taking turns randomly at branch points at the intersection of three cylindrulites. Isotropization in the interior follows *ca*. 0.1°C higher in temperature and occurs by nucleation and growth of disordered, non-birefringent regions. In some cases, adjacent cylindrulites disorder at slightly different temperatures, and there are indications that encirclement of clusters of cylindrulites by isotropized bands at their perimeter may promote earlier nucleation of disordering in their interiors. Inversion wall defects, which we had identified previously in these materials, generally persist above the isotropization temperature and are affected in a variety of ways as isotropic regions are nucleated: the inversion walls can be redirected to either side of an

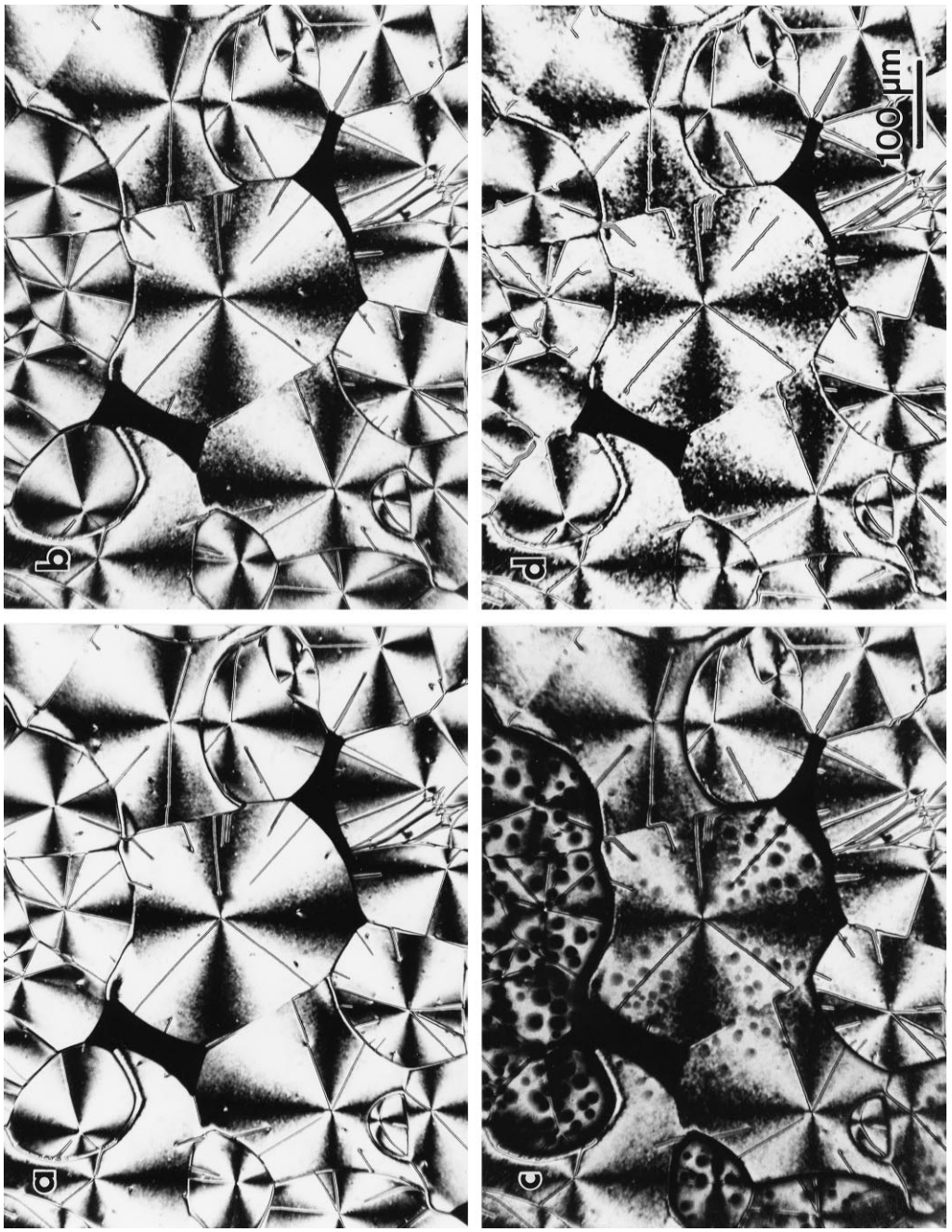

Figure 6 Sample of 25% LC exhibiting slight variations in isotropization behaviour of its cylindrulites. Originally at 25°C (a), then heated to 60°C (b) and then to 62.2°C (c), and finally cooled to room temperature from 62.2°C

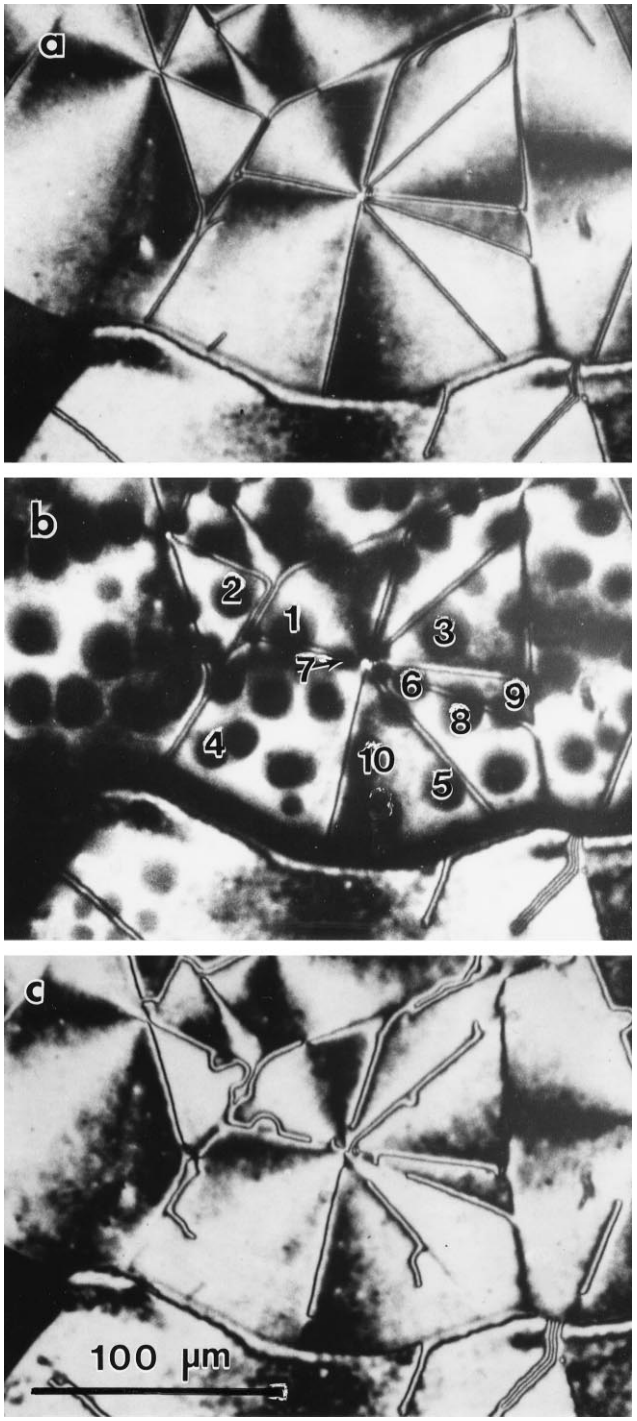

Figure 7 Effects of isotropization on inversion walls in cylindrulites of 25% LC (see text). (a) At 60°C, (b) at 62.2°C, and (c) cooled to room temperature from 62.2°C

isotropic domain with or without termination, they can be annihilated at that particular region, or they can remain unaffected.

REFERENCES

1. Fergason, J.L., *SID Tech. Dig.*, 1986, **16**, 68.
2. Drzaic, P.S., *J. Appl. Phys.*, 1986, **60**, 2142.
3. Doane, I.W., Vaz, N.A., Wu, B.-G and Zumer, S., *Appl. Phys. Lett.*, 1986, **48**, 269.
4. Doane, J.W., *MRS Bull.*, 1991, **1**, 22.
5. Drzaic, P.S., in *Liquid Crystal Dispersions.* World Scientific, New Jersey, 1995.
6. Sutherland, R.L., Natarajan, L.V., Tondiglia, V.P. and Bunning, T.J., *Chem. Mater.*, 1993, **5**, 1533.
7. Sutherland, R.L., Tondiglia, V.P., Natarajan, L.V., Bunning, T.J and Adams, W.W., *Appl. Phys. Lett.*, 1994, **64**, 1074.
8. Tondiglia, V.P., Natarajan, L.V., Sutherland, R.L., Bunning, T.J. and Adams, W.W., *Optics Lett.*, 1995, **20**, 1325.
9. West, J.L., *Mol. Cryst. Liq. Cryst.*, 1988, **157**, 427.
10. Smith, G.W., *Mol. Cryst. Liq. Cryst.*, 1991, **196**, 89.
11. Smith, G.W., *Phys. Rev. Lett.*, 1993, **70**, 198.
12. Hirai, Y., Niijima, S., Kumai, H. and Gunjima, T., *Rep. Res. Lab. Asahi Glass*, 1990, **40**, 285.
13. Boots, H.M.J., Kloosterboer, J.G., Serbutoviez, C. and Touwslager, F.J., *Macromolecules*, 1996, **29**, 7683.
14. Serbutoviez, C., Kloosterboer, J.G., Boots, H.M.J. and Touwslager, F.J., *Macromolecules*, 1996, **29**, 7690.
15. Serbutoviez, C., Kloosterboer, J.G., Boots, H.M.J., Paulissen, F.A.M.A and Touwslager, F.J., *Liq. Cryst.*, 1997, **22**, 145.
16. Srinivasarao, M. and Amundson, K.R., *ACS Polym Prepr.*, 1996, **37**(1), 200.
17. Neijzen, J.H.M., Boots, H.M.J., Paulissen, F.A.M.A., Van der Mark, M.B. and Cornelissen, H.J., *Liq. Cryst.*, 1997, **22**, 255.
18. Amundson, K.R., Van Blaaderen, A. and Wiltzius, P., *Phys. Rev. E*, 1997, **55**(2), 1646.
19. Lovinger, A.J., Amundson, K.R. and Davis, D.D., *Chem. Mater.*, 1994, **6**, 1726.
20. Lovinger, A. J., Amundson, K. R., Davis, D. D., in *Liquid Crystalline Polymer Systems: Technological Advances*, ACS Symp. Ser. 632, ed. A. I. Isayev, T. Kyu and S. Z. D. Cheng. American Chemical Society, Washington, 1996, p. 216.
21. Keith, H.D. and Padden, F.J. Jr., *J. Appl. Phys.*, 1963, **34**, 2409.
22. Keith, H.D. and Padden, F.J. Jr., *J. Appl. Phys.*, 1965, **35**, 1270–1286.
23. Wittmann, J.-C., Lotz, B., Candau, F. and Kovacs, A.J, *J. Polym. Sci., Polym. Phys. Ed.*, 1982, **20**, 1341.